# High-pressure synthesis, crystal structure, and structural relationship of the first ytterbium fluoride borate $Yb_5(BO_3)_2F_9$

Almut Haberer, Hubert Huppertz *

Institut für Allgemeine, Anorganische und Theoretische Chemie, Leopold-Franzens-Universität Innsbruck, Innrain 52a, A-6020 Innsbruck, Austria

## ARTICLE INFO

## ABSTRACT

$Yb_5(BO_3)_2F_9$ was synthesized under high-pressure/high-temperature conditions in a Walker-type multianvil apparatus at 7.5 GPa and 1100 °C, representing the first known ytterbium fluoride borate. The compound exhibits isolated $BO_3$-groups next to ytterbium cations and fluoride anions, showing a structure closely related to the other known rare-earth fluoride borates $RE_3(BO_3)_2F_3$ ($RE$ = Sm, Eu, Gd) and $Gd_2(BO_3)F_3$. Monoclinic $Yb_5(BO_3)_2F_9$ crystallizes in space group $C2/c$ with the lattice parameters $a = 2028.2(4)$ pm, $b = 602.5(2)$ pm, $c = 820.4(2)$ pm, and $\beta = 100.63(3)°$ ($Z = 4$). Three different ytterbium cations can be identified in the crystal structure, each coordinated by nine fluoride and oxygen anions. None of the five crystallographically independent fluoride ions is coordinated by boron atoms, solely by trigonally-planar arranged ytterbium cations. In close proximity to the above mentioned compounds $RE_3(BO_3)_2F_3$ ($RE$ = Sm, Eu, Gd) and $Gd_2(BO_3)F_3$, $Yb_5(BO_3)_2F_9$ can be described via alternating layers with the formal compositions "$YbBO_3$" and "$YbF_3$" in the $bc$-plane.

## 1. Introduction

In the past years, the field of rare-earth borates could be extended by the application of high-pressure/high-temperature techniques, leading to a large variety of new compounds, for example the rare-earth borates $RE_4B_6O_{15}$ ($RE$ = Dy, Ho) [1–3], $\alpha$-$RE_2B_4O_9$ ($RE$ = Sm–Ho) [4–6], $\beta$-$RE_2B_4O_9$ ($RE$ = Gd [7], Dy [8]), $Pr_4B_{10}O_{21}$ [9], and the *meta*-borates $\delta$-$RE(BO_2)_3$ ($RE$ = La, Ce) [10,11].

Borates, being glass formers in general, show an increasing willingness to crystallize under pressure. This kind of pressure-induced crystallization can be observed in $\beta$-$SnB_4O_7$ [12], $\beta$-$ZrB_2O_5$ [13], or $\beta$-$HfB_2O_5$ [14]. Also fluoroborates tend to form glasses with interesting optical properties. While borate glasses can be used for vacuum ultraviolet (VUV) optics, the addition of fluorine enlarges the optical gap [15]. We start now to investigate fluoro- and fluoride borates under high-pressure/high-temperature conditions, because they are likely yielding crystalline fluoroborate phases with interesting optical properties.

Until now, only the rare-earth fluoride borates $RE_3(BO_3)_2F_3$ ($RE$ = Sm, Eu, Gd) [16] and $Gd_2(BO_3)F_3$ [17] are known, which were synthesized by heating a stoichiometric mixture of $RE_2O_3$, $B_2O_3$, and $REF_3$ under ambient pressure conditions. The structure of $Gd_3(BO_3)_2F_3$ was solved from X-ray powder diffraction data, as suitable single crystals could not be found in the sample. In 2000, luminescence studies on $Eu_3(BO_3)_2F_3$ led to a disordered model of the structure [18]. In $Eu_3(BO_3)_2F_3$, three fluoride anions in the

structure were supposed to be partially replaced by oxoborate anions $BO_3^{3-}$, resulting in the formula $Eu_3(BO_3)_{2+x}F_{3-3x}$. This affects each of the three crystallographically different fluorides in the structure. In 2002, Müller-Bunz et al. [17] in vain tried to reproduce the isotypic compound $Gd_3(BO_3)_2F_3$. Instead of $Gd_3(BO_3)_2F_3$, the group yielded crystals of $Gd_2(BO_3)F_3$. But they found a close relationship between the two structures, both of which can be described via alternating layers of the formal compositions "$REBO_3$" and "$REF_3$" in the $bc$-plane. It should be emphasized that the crystal structures of the actual compounds $REBO_3$ and $REF_3$ cannot be compared with the structures of the layers, so that "$REBO_3$" and "$REF_3$" only stand for the formal compositions of the layers. The detection of disorder in crystals of $Gd_2(BO_3)F_3$ prompted to a new model of disorder, also applicable to $Eu_3(BO_3)_2F_3$.

In this article, we present the first ytterbium fluoride borate $Yb_5(BO_3)_2F_9$, obtained by high-pressure/high-temperature synthesis. The crystal structure of $Yb_5(BO_3)_2F_9$ can be developed from the structures mentioned above, showing alternating layers of the formal compositions "$YbBO_3$" and "$YbF_3$". We found disorder in parts of the structure, too, which might be explained along the model of disorder, proposed by Müller-Bunz et al. In the following, synthesis, structural details, and structural relationships of the new compound $Yb_5(BO_3)_2F_9$ are reported.
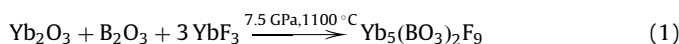
## 2. Experimental section

According to Eq. (1), the synthesis of $Yb_5(BO_3)_2F_9$ happened under high-pressure/high-temperature conditions, starting from

* Corresponding author. Fax: +435125072934.
E-mail address: hubert.huppertz@uibk.ac.at (H. Huppertz).

the binary oxides $Yb_2O_3$ and $B_2O_3$, as well as $YbF_3$:

$$Yb_2O_3 + B_2O_3 + 3\,YbF_3 \xrightarrow{7.5\,GPa,1100\,^\circ C} Yb_5(BO_3)_2F_9 \qquad (1)$$

A mixture of $Yb_2O_3$ (Smart Elements, 99.99%), $B_2O_3$ (Strem Chemicals, 99.9+%), and $YbF_3$ (Strem Chemicals, 99.9%) at a molar ratio of 1:1:3 (Eq. (1)) was ground up and filled into a boron nitride crucible (Henze BNP GmbH, HeBoSint® S10, Kempten, Germany). This crucible was placed into the center of an 18/11-assembly, which was compressed by eight tungsten carbide cubes (TSM-10 Ceratizit, Reutte, Austria). The details of preparing the assembly can be found in Refs. [19–23]. Pressure was applied by a multianvil device, based on a Walker-type module, and a 1000 ton press (both devices from the company Voggenreiter, Mainleus, Germany). The sample was compressed up to 7.5 GPa for 3 h, then heated to 1100 °C in 15 minutes and kept there for 20 minutes. Afterwards, the sample was cooled down to 850 °C in 20 minutes, followed by natural cooling down to room temperature after switching off heating. The decompression required 9 h. The recovered experimental MgO-octahedron (pressure transmitting medium, Ceramic Substrates & Components Ltd., Newport, Isle of Wight, UK) was broken apart and the sample carefully separated from the surrounding boron nitride crucible, obtaining colorless, air- and water-resistant, irregularly shaped crystals of $Yb_5(BO_3)_2F_9$.

## 3. Crystal structure analysis

The sample was characterized by powder X-ray diffraction, which was performed in transmission geometry on a flat sample of the reaction product, using a STOE STADI P powder diffractometer with $MoK\alpha_1$ radiation (Ge monochromator, $\lambda = 71.073$ pm). Fig. 1 shows a powder pattern of the sample (top), exhibiting $Yb_5(BO_3)_2F_9$, as well as reflections of another still unknown side product, marked with lines. The experimental powder pattern tallies well with the theoretical pattern (bottom), simulated from single-crystal data. Indexing the reflections of the ytterbium fluoride borate, we got the parameters $a = 2028.0(2)$ pm, $b = 602.5(3)$ pm, and $c = 821.5(5)$ pm, with $\beta = 100.62(5)^\circ$ and a volume of $986.6(7)$ Å$^3$. This confirms the lattice parameters, obtained from single-crystal X-ray diffraction (Table 1).

The intensity data of a single crystal of $Yb_5(BO_3)_2F_9$ were collected at room temperature by use of a Kappa CCD diffracto-meter (Bruker AXS/Nonius, Karlsruhe), equipped with a Miracol Fiber Optics Collimator and a Nonius FR590 generator (graphite-monochromatized $MoK\alpha_1$ radiation, $\lambda = 71.073$ pm). Additionally, the data set was subjected to a numerical absorption correction (HABITUS [24]). All relevant details of the data collection and evaluation are listed in Table 1.

Structure solution and parameter refinement (full-matrix least-squares against $F^2$) were successfully performed, using the SHELX-97 software suite [25,26] with anisotropic atomic displacement parameters for all atoms. According to the systematic extinctions, the monoclinic space groups $C2/c$ and $Cc$ were derived. The structure solution in $C2/c$ (no. 15) succeeded. The final difference Fourier syntheses did not reveal any significant residual peaks in all refinements. The positional parameters of the refinements, anisotropic displacement parameters, interatomic distances, and interatomic angles are listed in the Tables 2–5. Further information of the crystal structure is available from the Fachinformationszentrum Karlsruhe (crysdata@fiz-karlsruhe.de), D-76344 Eggenstein-Leopoldshafen (Germany), quoting the Registry no. CSD-420182.
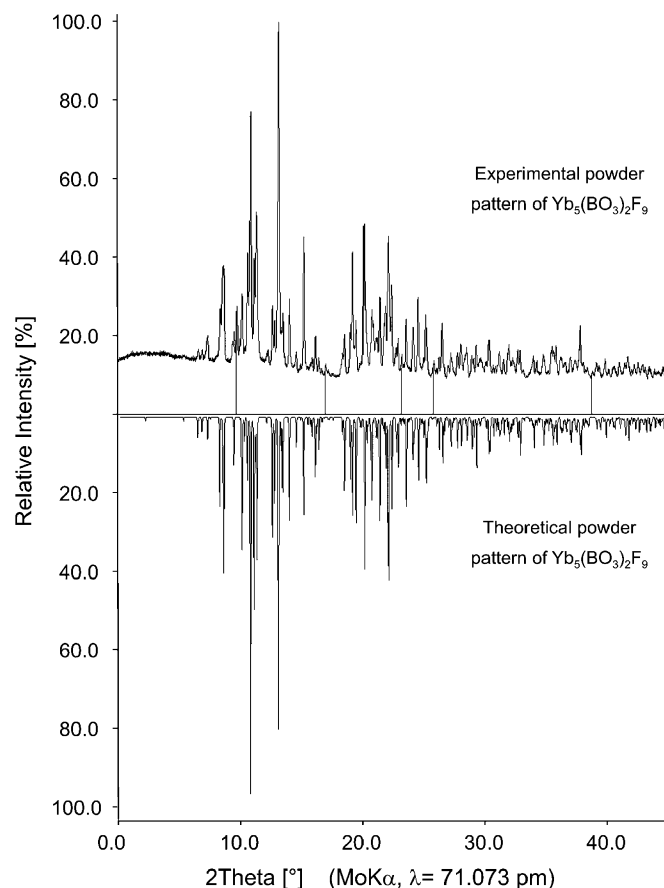


**Fig. 1.** Top: Experimental powder pattern of $Yb_5(BO_3)_2F_9$; reflections of an unknown phase are indicated with lines. Bottom: theoretical powder pattern of $Yb_5(BO_3)_2F_9$, based on single-crystal diffraction data.

## 4. Results and discussion

### 4.1. Crystal structure of $Yb_5(BO_3)_2F_9$

The structure of $Yb_5(BO_3)_2F_9$ consists of isolated $BO_3$-groups, ytterbium cations, and fluoride anions (Fig. 2). As shown in Fig. 3, the structure can be described via alternating layers of the formal compositions "$YbBO_3$" and "$YbF_3$", spreading into the $bc$-plane. The layers are labeled in a way, that reveals their relationship to other rare-earth fluoride borates, as explained below.

There are three crystallographically independent $Yb^{3+}$ ions in the structure, which are nine-fold coordinated by oxygen and fluorine (Fig. 4). Yb1 and Yb3 have got four oxide and five fluoride ions in the coordination sphere, whereas Yb2 is surrounded by three oxide and six fluoride ions. The average interatomic distance Yb–O with 234.2 pm is in the same range, but shorter than the average Gd–O distance of ninefold coordinated $Gd^{3+}$ in $Gd_2[BO_3]F_3$ (242.2 pm [17]), as we would expect from the smaller ionic radius of $Yb^{3+}$.

Each one of the five fluoride ions in $Yb_5(BO_3)_2F_9$ is coordinated by three ytterbium ions (Fig. 5). The bond lengths in Table 4 range between 218.6(4) and 294.2(5) pm, being in the same region as the bond lengths of threefold-coordinated fluoride ions in $YbF_3$ (203.9–284.7 pm) [27]. The Yb–F angles sum up to $\sim120^\circ$ (Table 5), as expected from trigonal-planar geometry.

Regarding the $BO_3$-group in the structure, the average B–O distance is 142.7 pm (Table 4). This is fairly large for interatomic distances in $BO_3$-groups, which are usually in a range

**Table 1**
Crystal data and structure refinement of $Yb_5(BO_3)_2F_9$.

| | |
|---|---|
| Empirical formula | $Yb_5(BO_3)_2F_9$ |
| Molar mass ($g\,mol^{-1}$) | 1153.82 |
| Crystal system | Monoclinic |
| Space group | $C2/c$ (No. 15) |
| | |
| *Lattice parameters from powder data* | |
| Powder diffractometer | Stoe Stadi P |
| Radiation | $MoK\alpha_1$ ($\lambda = 71.073$ pm) |
| $a$ (pm) | 2028.0(2) |
| $b$ (pm) | 602.5(3) |
| $c$ (pm) | 821.5(5) |
| $\beta$ (deg.) | 100.62(5) |
| Volume ($\text{Å}^3$) | 986.6(7) |
| | |
| *Single-crystal data* | |
| Single-crystal diffractometer | Bruker AXS/Nonius Kappa CCD |
| Radiation | $MoK\alpha_1$ ($\lambda = 71.073$ pm) |
| $a$ (pm) | 2028.2(4) |
| $b$ (pm) | 602.5(2) |
| $c$ (pm) | 820.4(2) |
| $\beta$ (deg.) | 100.63(3) |
| Volume ($\text{Å}^3$) | 985.3(3) |
| | |
| Formula units per cell | $Z = 4$ |
| Temperature (K) | 293(2) |
| Calculated density ($g\,cm^{-3}$) | 7.778 |
| Crystal size ($mm^3$) | $0.04 \times 0.03 \times 0.02$ |
| Absorption coefficient ($mm^{-1}$) | 47.163 |
| $F$ (000) | 1956 |
| $\theta$ range (deg.) | $2.04 \leqslant \theta \leqslant 32.49$ |
| Range in $h\,k\,l$ | $-28/30, \pm 9, \pm 12$ |
| Total no. of reflections | 13 200 |
| Independent reflections | 1784 ($R_{int} = 0.1157$) |
| Reflections with $I > 2\sigma(I)$ | 1604 ($R_\sigma = 0.0494$) |
| Data/parameters | 1784/102 |
| Absorption correction | numerical (HABITUS [24]) |
| Transm. ratio (min/max) | 0.1987/0.3881 |
| Goodness-of-fit ($F^2$) | 1.065 |
| Final $R$ indices ($I > 2\sigma(I)$) | $R1 = 0.0294$ |
| | $wR2 = 0.0638$ |
| $R$ indices (all data) | $R1 = 0.0352$ |
| | $wR2 = 0.0658$ |
| Largest differ. peak, deepest hole ($e/\text{Å}^3$) | $2.07/-2.58$ |

**Table 2**
Atomic coordinates and isotropic equivalent displacement parameters ($U_{eq}/\text{Å}^2$) for $Yb_5(BO_3)_2F_9$ (space group: $C2/c$).

| Atom | Wyckoff site | $x$ | $y$ | $z$ | $U_{eq}$ |
|---|---|---|---|---|---|
| Yb1 | 8f | 0.30685(2) | 0.12006(4) | 0.18004(3) | 0.00705(9) |
| Yb2 | 8f | 0.39063(2) | 0.38939(4) | 0.59241(3) | 0.00896(9) |
| Yb3 | 4e | 1/2 | 0.11101(7) | 1/4 | 0.0088(2) |
| B1 | 8f | 0.3880(5) | 0.905(2) | 0.437(2) | 0.020(2) |
| O1 | 8f | 0.4094(2) | 0.7587(8) | 0.5663(5) | 0.0071(8) |
| O2 | 8f | 0.3375(3) | 0.072(2) | 0.4630(6) | 0.014(2) |
| O3 | 8f | 0.4077(3) | 0.1053(8) | 0.7801(6) | 0.0106(9) |
| F1 | 8f | 0.2897(2) | 0.4241(7) | 0.0198(5) | 0.0109(7) |
| F2 | 8f | 0.3689(2) | 0.4250(7) | 0.3138(5) | 0.0125(8) |
| F3 | 4e | 1/2 | 0.489(2) | 1/4 | 0.013(2) |
| F4 | 8f | 0.2735(2) | 0.7819(8) | 0.2172(5) | 0.0145(8) |
| F5 | 8f | 0.4690(2) | 0.1870(9) | 0.5119(6) | 0.021(2) |

$U_{eq}$ is defined as one-third of the trace of the orthogonalized $U_{ij}$ tensor.

**Table 3**
Anisotropic displacement parameters ($U_{ij}/\text{Å}^2$) for $Yb_5(BO_3)_2F_9$ (space group: $C2/c$).

| Atom | $U_{11}$ | $U_{22}$ | $U_{33}$ | $U_{12}$ | $U_{13}$ | $U_{23}$ |
|---|---|---|---|---|---|---|
| Yb1 | 0.0088(2) | 0.0047(2) | 0.0075(2) | 0.00016(9) | 0.00110(9) | $-0.00031(8)$ |
| Yb2 | 0.0160(2) | 0.0048(2) | 0.0058(2) | 0.00300(9) | 0.00142(9) | $-0.00021(8)$ |
| Yb3 | 0.0061(2) | 0.0095(2) | 0.0106(2) | 0 | 0.0010(2) | 0 |
| B1 | 0.020(4) | 0.023(4) | 0.017(4) | $-0.002(3)$ | 0.001(3) | 0.001(3) |
| O1 | 0.010(2) | 0.006(2) | 0.005(2) | $-0.000(2)$ | 0.000(2) | $-0.001(2)$ |
| O2 | 0.011(2) | 0.022(3) | 0.008(2) | $-0.011(2)$ | $-0.005(2)$ | 0.003(2) |
| O3 | 0.015(2) | 0.009(2) | 0.006(2) | 0.004(2) | $-0.001(2)$ | $-0.001(2)$ |
| F1 | 0.012(2) | 0.010(2) | 0.010(2) | $-0.002(2)$ | $-0.001(2)$ | $-0.001(2)$ |
| F2 | 0.018(2) | 0.012(2) | 0.008(2) | $-0.004(2)$ | 0.003(2) | $-0.005(2)$ |
| F3 | 0.013(3) | 0.012(3) | 0.014(3) | 0 | $-0.001(2)$ | 0 |
| F4 | 0.013(2) | 0.013(2) | 0.017(2) | $-0.004(2)$ | 0.001(2) | 0.005(2) |
| F5 | 0.018(2) | 0.019(2) | 0.026(2) | $-0.002(2)$ | 0.006(2) | $-0.008(2)$ |

**Table 4**
Interatomic distances (pm) in $Yb_5(BO_3)_2F_9$, calculated with the single-crystal lattice parameters.

| | | | | | |
|---|---|---|---|---|---|
| Yb1–O2a | 230.2(5) | Yb2–O1 | 227.4(5) | Yb3–O1 | 228.9(4) (2×) |
| Yb1–O2b | 230.8(5) | Yb2–O3 | 228.6(5) | Yb3–O3 | 233.1(5) (2×) |
| Yb1–O3 | 246.6(5) | Yb2–O2 | 235.2(5) | Yb3–F3 | 227.8(6) |
| Yb1–O1 | 253.9(5) | Yb2–F5 | 219.9(5) | Yb3–F5a | 239.2(5) (2×) |
| Yb1–F4a | 218.6(4) | Yb2–F2a | 224.4(4) | Yb3–F5b | 264.2(5) (2×) |
| Yb1–F4b | 219.7(4) | Yb2–F2b | 225.7(4) | | |
| Yb1–F1a | 224.4(4) | Yb2–F1 | 231.5(4) | | |
| Yb1–F1b | 232.6(4) | Yb2–F3 | 246.4(2) | | |
| Yb1–F2 | 237.8(4) | Yb2–F4 | 294.2(5) | | |
| | | | | | |
| B1–O1 | 138.7(10) | | | | |
| B1–O3 | 141.5(11) | | | | |
| B1–O2 | 148.0(12) | $\varnothing = 142.7$ | | | |
| | | | | | |
| F1–Yb1a | 224.4(5) | F2–Yb2a | 224.4(5) | F3–Yb3 | 227.8(7) |
| F1–Yb2 | 231.5(5) | F2–Yb2b | 225.7(4) | F3–Yb2a | 246.4(2) (2×) |
| F1–Yb1b | 232.6(5) | F2–Yb1 | 237.8(4) | | |
| | | | | | |
| F4–Yb1a | 218.6(5) | F5–Yb2a | 219.9(5) | | |
| F4–Yb2 | 219.7(5) | F5–Yb2b | 239.2(5) | | |
| F4–Yb1b | 294.2(5) | F5–Yb1 | 264.2(6) | | |

**Table 5**
Interatomic angles (deg.) in $Yb_5(BO_3)_2F_9$, calculated with the single-crystal lattice parameters.

| | | | | | |
|---|---|---|---|---|---|
| O1–B1–O3 | 124.6(8) | Yb1a–F1–Yb2 | 102.2(2) | Yb2a–F2–Yb2b | 146.7(2) |
| O1–B1–O2 | 116.5(7) | Yb1a–F1–Yb1b | 109.8(2) | Yb2a–F2–Yb1 | 100.2(2) |
| O3–B1–O2 | 118.7(7) | Yb2–F1–Yb1b | 145.4(3) | Yb2b–F2–Yb1 | 112.4(2) |
| | | | | | |
| | $\varnothing = 119.9$ | | $\varnothing = 119.1$ | | $\varnothing = 119.8$ |
| | | | | | |
| Yb3–F3–Yb2a | 107.3(2) | Yb1a–F4–Yb1b | 137.6(2) | Yb2–F5–Yb3a | 134.5(2) |
| Yb3–F3–Yb2b | 107.3(2) | Yb1a–F4–Yb2 | 89.3(2) | Yb2–F5–Yb3b | 104.0(2) |
| Yb2a–F3–Yb2b | 145.4(3) | Yb1b–F4–Yb2 | 133.0(2) | Yb3a–F5–Yb3b | 117.9(2) |
| | | | | | |
| | $\varnothing = 120.0$ | | $\varnothing = 120.0$ | | $\varnothing = 118.8$ |

around 137 pm, e.g. in borates with calcite structure ($AlBO_3$ (137.96(4) pm) [28], $\beta$-$YbBO_3$ (137.8(4) pm) [29], and $FeBO_3$ (137.9(2) pm) [30]). The bond lengths B–O1 (138.7(10) pm) and B–O3 (141.5(11) pm) show high standard deviations, but normal values. So the large average B–O distance is mainly due to the large distance B–O2 with 148.0(12) pm, exhibiting a high standard deviation, too. This holds also true for the O–B–O angles, where the large angle O1–B1–O3 (124.6(8)°) underlines the displacement of the boron atom from the center of the $BO_3$ triangle. High standard deviations can be observed, too, for the isotropic and anisotropic displacement parameters of B1 and O2. All these findings might be evoked by a possible disorder in the $BO_3$-group (Table 3). This was also observed in $Gd_3(BO_3)_2F_3$ [16] and $Gd_2(BO_3)F_3$ [17] and will be discussed in the following section.

The formal layers in the *bc*-plane of Yb$_5$(BO$_3$)$_2$F$_9$ (Fig. 3) show the formal compositions "YbBO$_3$" and "YbF$_3$". In detail, the layer B in Fig. 3 formally comprises Yb3 in strings of YbFF$_{4/2}$, running along [001], as shown in Fig. 6. Layer C has the formal composition (Yb2)BO$_3$, depicted in Fig. 7 (left). Layer E (Fig. 7, right) has got the same composition, but a shifted arrangement by $\frac{1}{2}$ along the *b*-axis compared to layer C. A corrugated sheet with Yb1 in the formal composition YbF$_{6/2}$ builds up layer D (Fig. 8). The arrangement of the Yb cations in the layers explains the similar coordination spheres of Yb1 and Yb3 (4 O, 5 F), and the differing coordination of Yb2 (3 O, 6 F). Simply adding the formal constitutions of the layers, illustrated in Fig. 3, (B+B' = 2 YbF$_3$, C+C'+E+E' = 4 YbBO$_3$, D+D' = 4 YbF$_3$), we come to the formula 4 YbBO$_3 \cdot$ 6 YbF$_3$ = 2 Yb$_5$(BO$_3$)$_2$F$_9$.

The calculations of the charge distribution of the atoms in Yb$_5$(BO$_3$)$_2$F$_9$ via bond valence sums ($\Sigma V$) with VaList (bond valence calculation and listing) [31] and with the CHARDI concept ($\Sigma Q$) [32–34] confirm the formal valence states in the fluoride borate (Table 6). The low value of 2.59 for B1 in the VaList calculation is caused by the extraordinary long B–O2 bond, which is not adequately considered in the bond-length/bond-strength calculations. CHARDI calculations provide the expected value of 2.99 for B1.

Furthermore, we calculated the Madelung Part of Lattice Energy (MAPLE) values [35–37] for Yb$_5$(BO$_3$)$_2$F$_9$ in order to compare them with the MAPLE values of the high-pressure modification of Yb$_2$O$_3$ [38], of the ambient-pressure modification of B$_2$O$_3$ (B$_2$O$_3$–I) [39], and of YbF$_3$ [27]. The additive potential of the MAPLE values allows the calculation of hypothetical values for Yb$_5$(BO$_3$)$_2$F$_9$, starting from binary oxides and fluorides. As a result, we obtained a value of 53 819 kJ/mol in comparison to 53 661 kJ/mol (deviation: 0.3%), starting from the binary components [1 × Yb$_2$O$_3$ (15 590 kJ/mol) + 1 × B$_2$O$_3$–I (20 626 kJ/mol) + 3 × YbF$_3$ (17 445 kJ/mol)].

### 4.2. Comparison of Yb$_5$(BO$_3$)$_2$F$_9$ to other rare-earth fluoride borates

Besides Yb$_5$(BO$_3$)$_2$F$_9$, the only other known rare-earth fluoride borates are *RE*$_3$(BO$_3$)$_2$F$_3$ (*RE* = Sm, Eu, Gd) [16] and Gd$_2$(BO$_3$)F$_3$ [17]. Both structures show a quite similar constitution of formal rare-earth borate and fluoride layers (Fig. 9 left and middle). Müller-Bunz et al. realized that the duplicating of the formula Gd$_2$(BO$_3$)F$_3$ leads to Gd$_4$(BO$_3$)$_2$F$_6$, which can be written as Gd$_3$(BO$_3$)$_2$F$_3 \cdot$ GdF$_3$ [17]. This illustrates the relationship of the two structures: by inserting the GdF$_3$ layer D in layer A' of Gd$_3$(BO$_3$)$_2$F$_3$, there emerge the layers C and C'.

Looking at Yb$_5$(BO$_3$)$_2$F$_9$, we found that it can be written as Yb$_3$(BO$_3$)$_2$F$_3 \cdot$ 2 YbF$_3$. In analogy to the insertion step mentioned above, an additional YbF$_3$ layer D can be found in the structure, splitting the remaining layer A of Gd$_2$(BO$_3$)F$_3$ (Fig. 9 middle) into the layers E and E' in Yb$_5$(BO$_3$)$_2$F$_9$ (Fig. 9 right).

The insertion of *RE*F$_3$ layers into the structure of Gd$_3$(BO$_3$)$_2$F$_3$ stretches the *a*-axis, ranging from 1253.4(1) pm in Gd$_3$(BO$_3$)$_2$F$_3$ via
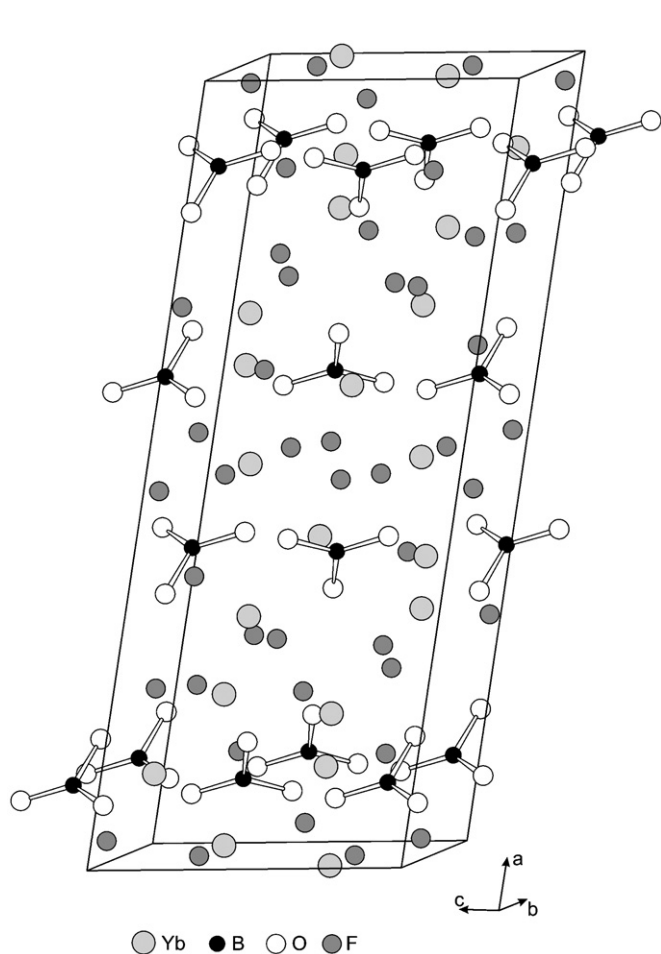


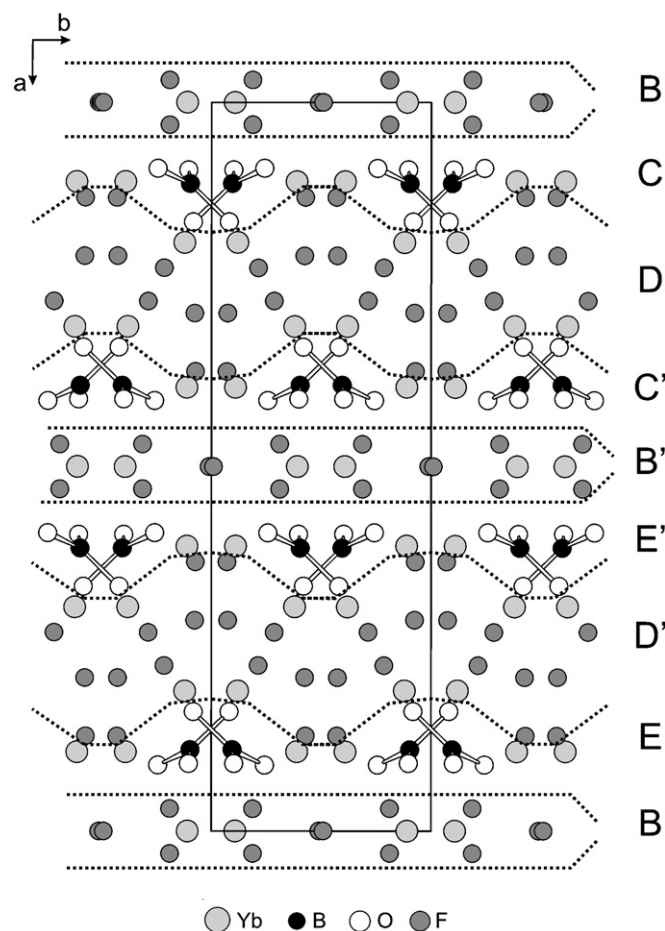**Fig. 2.** Crystal structure of Yb$_5$(BO$_3$)$_2$F$_9$, showing isolated BO$_3$-groups.



**Fig. 3.** Structure of Yb$_5$(BO$_3$)$_2$F$_9$, depicting alternating layers in the *bc*-plane with the formal compositions "YbBO$_3$" and "YbF$_3$".
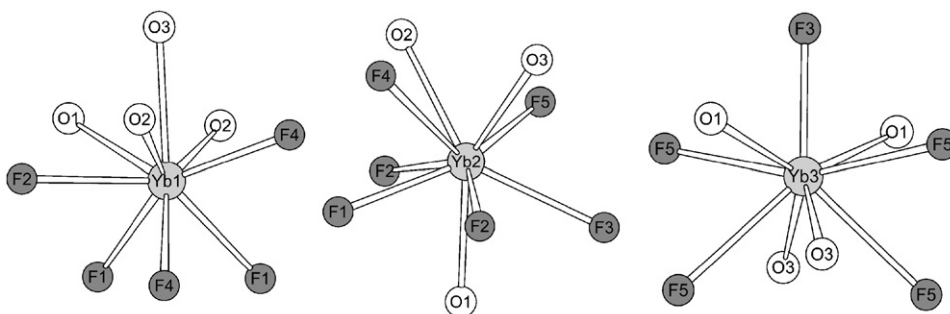
**Fig. 4.** Coordination spheres of the three $Yb^{3+}$ ions in $Yb_5(BO_3)_2F_9$.
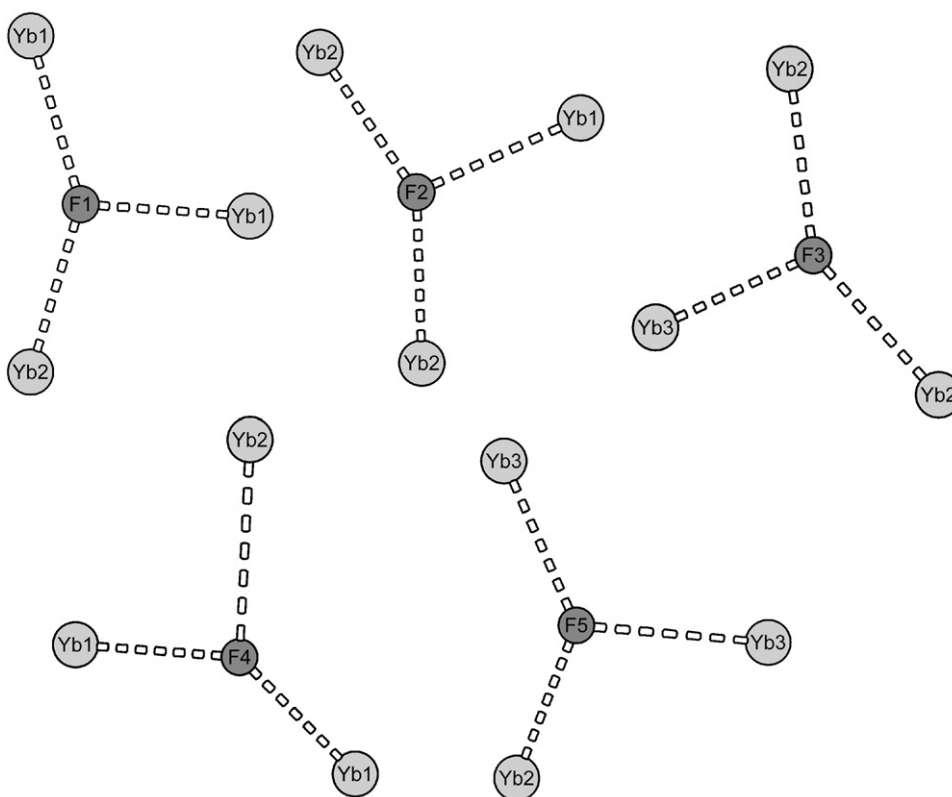


**Fig. 5.** Trigonal coordination of fluoride ions in $Yb_5(BO_3)_2F_9$.

1637.2(1) pm in $Gd_2(BO_3)F_3$ to 2028.2(4) pm in $Yb_5(BO_3)_2F_9$. Compared to the $a$-axis, the other cell edges differ only marginally, as depicted in Fig. 10. Due to the smaller ionic radius of $Yb^{3+}$, they shrink slightly in $Yb_5(BO_3)_2F_9$.

The boron position in $Gd_3(BO_3)_2F_3$ could not be refined by Corbel et al. [16]. Studying the fluorescence properties of $Eu_3(BO_3)_2F_3$, Antic-Fidancev et al. [18] found some evidence for a disorder in the $BO_3$-group of the structure. When measuring crystals of $Gd_2(BO_3)F_3$, Müller-Bunz et al. discovered that there is more than one possible position for the boron atoms in the structure: if you switch the positions of an oxygen ion of the $BO_3$-group and an adjacent fluoride ion, the location of the $BO_3$-group changes. A more detailed description of the model of disorder can be found in Ref. [17]. We simulated this for $Yb_5(BO_3)_2F_9$, splitted the boron position manually and resulted in

acceptable B2–O distances, even though we did not find evidence for a second boron position in our crystals. So, probably, the same kind of disorder, found in $Gd_2(BO_3)F_3$ and postulated for $Gd_3(BO_3)_2F_3$, exists (at least to a small amount) in $Yb_5(BO_3)_2F_9$ as well. This would explain the large standard deviations of the structural parameters in the $BO_3$-group.

### 4.3. IR spectroscopy

The infrared spectrum of $Yb_5(BO_3)_2F_9$ was recorded on a Nicolet 5700 FT-IR spectrometer, scanning a range from 400 to $4000 cm^{-1}$. Before measuring, the sample was thoroughly dried under high vacuum for several days. Fig. 10 shows the complete spectral region between 400 and $4000 cm^{-1}$. The absorptions in

the area of $2000\,\mathrm{cm}^{-1}$ are evoked by the diamond window of the spectrometer and thus part of the background of the measurement. The absorptions between 1200 and $1400\,\mathrm{cm}^{-1}$, between 600 and $800\,\mathrm{cm}^{-1}$ and below $500\,\mathrm{cm}^{-1}$ characterize triangular $BO_3$-groups as in $\lambda$-$LaBO_3$ [40], H-$LaBO_3$ [41], or $EuB_2O_4$ [42]. In the region of $3000$–$3500\,\mathrm{cm}^{-1}$, absorption peaks could not be detected. Peaks at those wavelengths can be assigned to OH-groups and typically reveal water-containing borates. On the basis of this IR measurement, we can exclude OH-groups in $Yb_5(BO_3)_2F_9$ (Fig. 11).



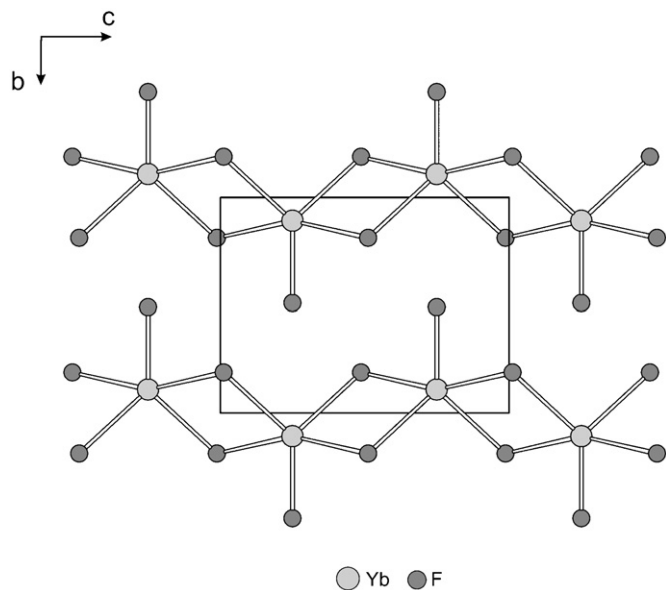Fig. 6. View of layer B in the *bc*-plane of $Yb_5(BO_3)_2F_9$, comprising Yb3 in Yb–F-strings with the formal composition $YbFF_{4/2}$.
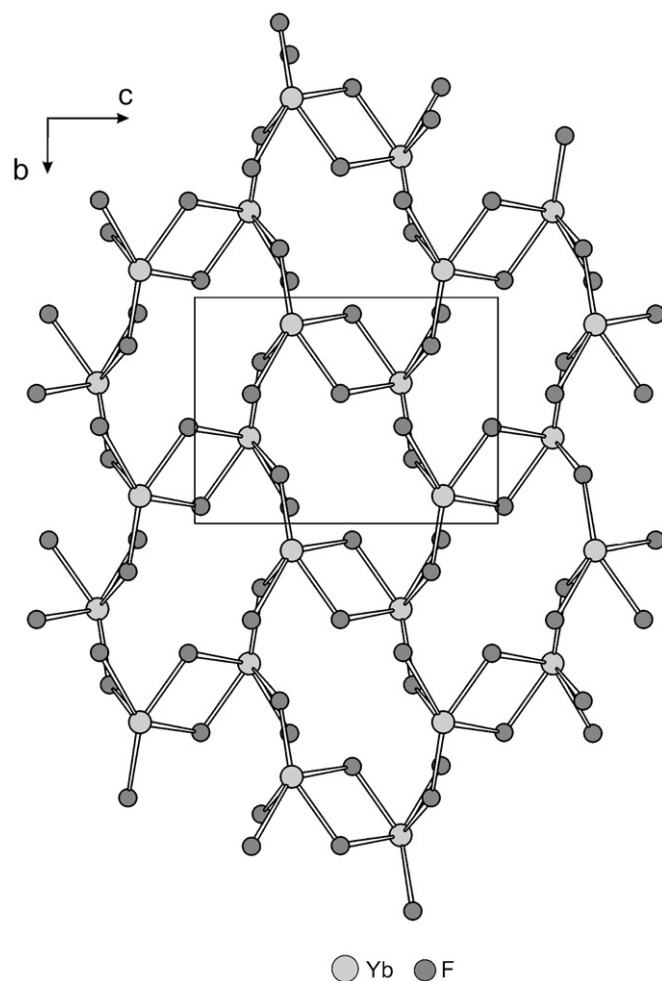


Fig. 8. Corrugated sheet with Yb1 in the formal composition $YbF_{6/2}$ in the *bc*-plane, building up layer D in $Yb_5(BO_3)_2F_9$.
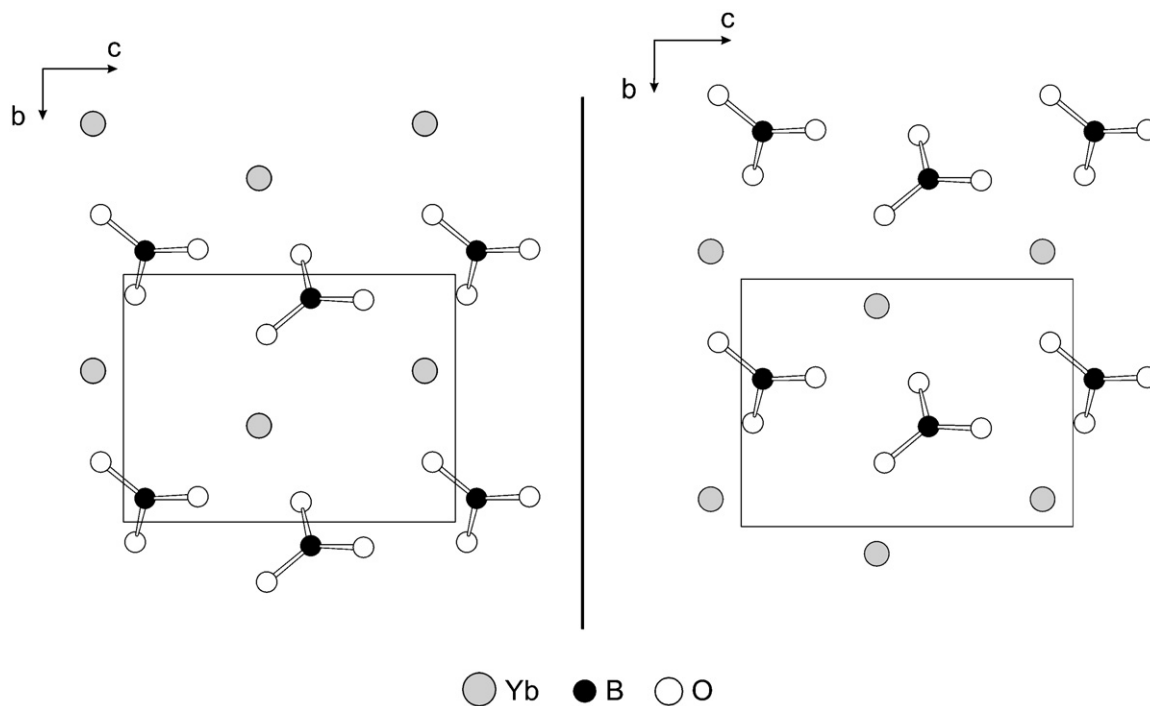


Fig. 7. Layers C (left) and E (right) in the *bc*-plane of $Yb_5(BO_3)_2F_9$, exhibiting the formal composition $(Yb2)BO_3$.

**Table 6**
Charge distribution in $Yb_5(BO_3)_2F_9$, calculated with VaList ($\Sigma V$) [31] and the CHARDI concept ($\Sigma Q$) [32–34].

|            | Yb1   | Yb2   | Yb3   | B1    |       |       |       |       |
| ---------- | ----- | ----- | ----- | ----- | ----- | ----- | ----- | ----- |
| $\Sigma V$ | 3.04  | 2.91  | 2.66  | 2.59  |       |       |       |       |
| $\Sigma Q$ | 3.05  | 2.94  | 3.05  | 2.99  |       |       |       |       |
|            | O1    | O2    | O3    | F1    | F2    | F3    | F4    | F5    |
| $\Sigma V$ | −2.02 | −1.89 | −1.94 | −0.97 | −0.98 | −0.74 | −0.91 | −0.79 |
| $\Sigma Q$ | −2.15 | −1.79 | −2.03 | −1.10 | −1.13 | −0.87 | −0.92 | −0.94 |
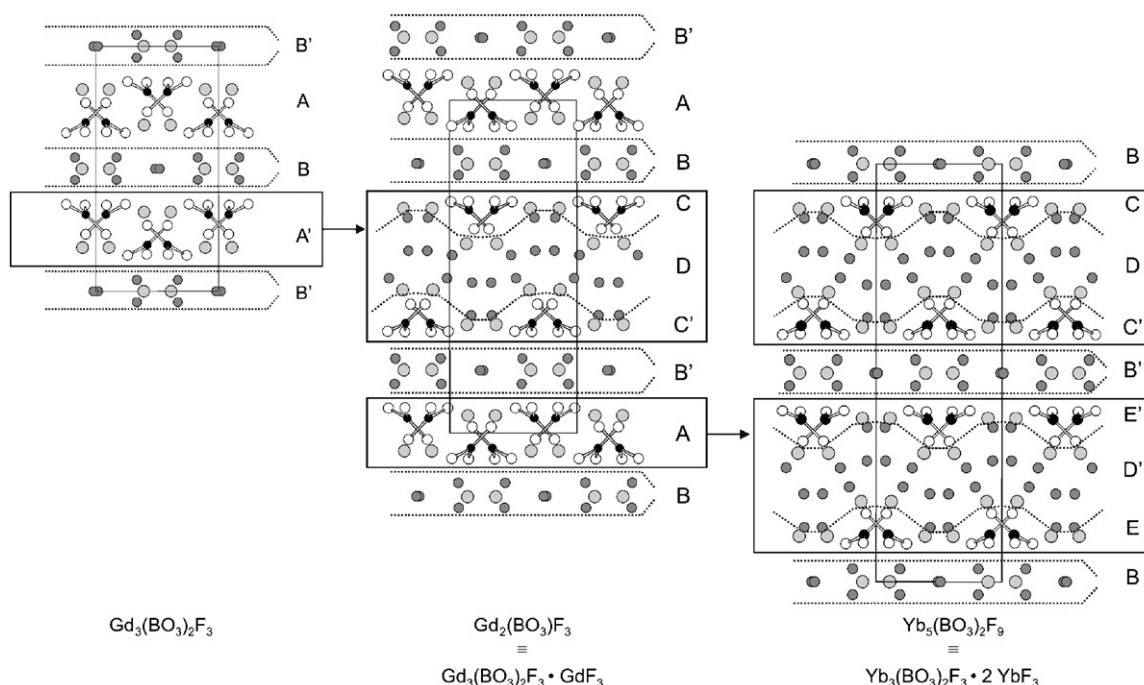


**Fig. 9.** Comparison of the structures of $Gd_3(BO_3)_2F_3$ (left), $Gd_2(BO_3)F_3$ (middle) and $Yb_5(BO_3)_2F_9$ (right). The splitting of layer A′ into layers C, D, and C′ is depicted in the left part; splitting of layer A into layers E, D′, and E′ is shown on the right ($RE$ = light gray spheres, B = black spheres, O = hollow spheres, F = dark gray spheres).
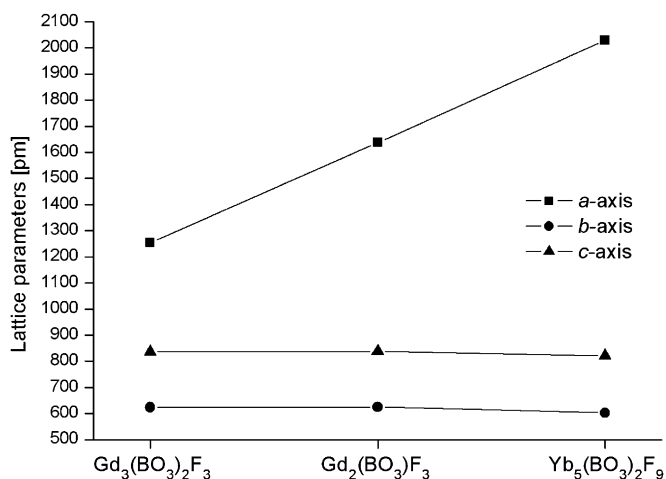


**Fig. 10.** Lattice parameters of $Gd_3(BO_3)_2F_3$ (left), $Gd_2(BO_3)F_3$ (middle), and $Yb_5(BO_3)_2F_9$ (right).

## 5. Conclusions

In this article, we described the high-pressure synthesis and crystal structure of the first ytterbium fluoride borate $Yb_5(BO_3)_2F_9$. It shows a structure closely related to the known gadolinium fluoride borates $Gd_3(BO_3)_2F_3$ and $Gd_2(BO_3)F_3$. We found some evidence of disorder in the $BO_3$-group of $Yb_5(BO_3)_2F_9$; nevertheless, we can neither confirm nor refute the disorder model existing for the gadolinium fluoride borates. The synthesis of similar structures, starting from oxides and fluorides of different rare-earth cations, can—as we hope—make understand the actual formation of the structure and will be the object of our forthcoming studies. Investigations concerning optical properties of our fluoride borate, especially a possible enlargement of the optical gap, will be performed in the future.

Another point, stimulating our interest, are higher pressures on $Yb_5(BO_3)_2F_9$ to transform the $BO_3$-groups of the structure into $BO_4$-tetrahedra. This already succeeded and led to a new structure exhibiting very interesting properties [43].
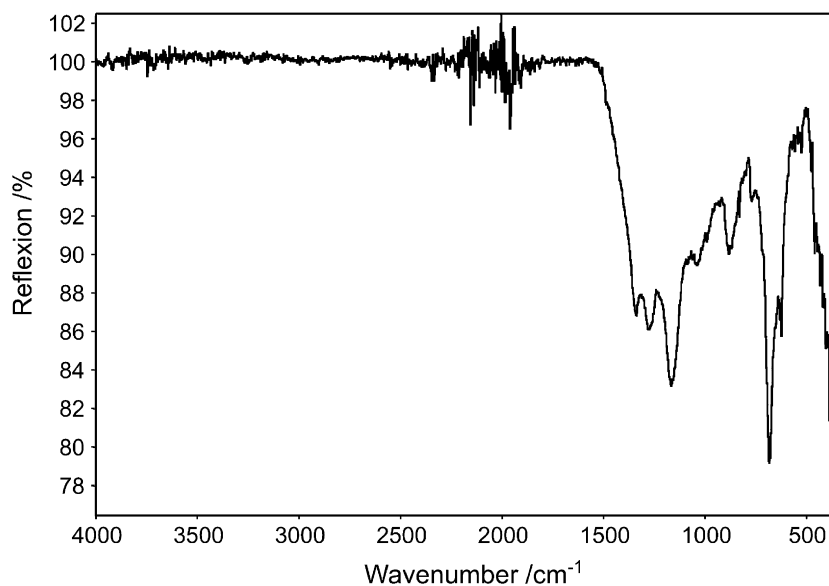
**Fig. 11.** IR spectrum of $Yb_5(BO_3)_2F_9$.

## Acknowledgments

## Appendix A. Supplementary materials

Supplementary data associated with this article can be found in the online version at: doi:10.1016/j.jssc.2009.01.023.

## References

[1] H. Huppertz, B. von der Eltz, J. Am. Chem. Soc. 124 (2002) 9376.
[2] H. Huppertz, Z. Naturforsch. B 58 (2003) 278.
[3] H. Huppertz, H. Emme, J. Phys. Condens. Matter 16 (2004) 1283.
[4] H. Emme, H. Huppertz, Z. Anorg. Allg. Chem. 628 (2002) 2165.
[5] H. Emme, H. Huppertz, Chem. Eur. J. 9 (2003) 3623.
[6] H. Emme, H. Huppertz, Acta Crystallogr. C 61 (2005) i29.
[7] H. Emme, H. Huppertz, Acta Crystallogr. C 61 (2005) i23.
[8] H. Huppertz, S. Altmannshofer, G. Heymann, J. Solid State Chem. 170 (2003) 320.
[9] A. Haberer, G. Heymann, H. Huppertz, J. Solid State Chem. 180 (2007) 1595.
[10] G. Heymann, T. Soltner, H. Huppertz, Solid State Sci. 8 (2006) 821.
[11] A. Haberer, G. Heymann, H. Huppertz, Z. Naturforsch. B 62 (2007) 759.
[12] J.S. Knyrim, F.M. Schappacher, R. Pöttgen, J. Schmedt auf der Günne, D. Johrendt, H. Huppertz, Chem. Mater. 19 (2007) 254.
[13] J.S. Knyrim, H. Huppertz, Z. Naturforsch. 63b (2008) 707.
[14] J.S. Knyrim, H. Huppertz, J. Solid State Chem. 180 (2007) 742.
[15] T. Suzuki, M. Hirano, H. Hosono, J. Appl. Phys. 91 (2002) 4149.
[16] G. Corbel, R. Retoux, M. Leblanc, J. Solid State Chem. 139 (1998) 52.
[17] H. Müller-Bunz, Th. Schleid, Z. Anorg. Allg. Chem. 628 (2002) 2750.
[18] E. Antic-Fidancev, G. Corbel, N. Mercier, M. Leblanc, J. Solid State Chem. 153 (2000) 270.
[19] D. Walker, M.A. Carpenter, C.M. Hitch, Am. Mineral 75 (1990) 1020.
[20] D. Walker, Am. Mineral 76 (1991) 1092.
[21] H. Huppertz, Z. Kristallogr. 219 (2004) 330.
[22] D.C. Rubie, Phase Transitions 68 (1999) 431.
[23] N. Kawai, S. Endo, Rev. Sci. Instrum. 8 (1970) 1178.
[24] W. Herrendorf, H. Bärnighausen, HABITUS, Universities of Karlsruhe and Giessen, Germany, 1993/1997.
[25] G.M. Sheldrick, SHELXS-97 and SHELXL-97, Program suite for the solution and refinement of crystal structures, University of Göttingen, Göttingen, Germany, 1997.
[26] G.M. Sheldrick, Acta Crystallogr. A 64 (2008) 112.
[27] A. Zalkin, D.H. Templeton, J. Am. Chem. Soc. 75 (1953) 2453.
[28] A. Vegas, Acta Crystallogr. B 33 (1977) 3607.
[29] H. Huppertz, Z. Naturforsch. B 56 (2001) 697.
[30] R. Diehl, Solid State Commun. 17 (1975) 743.
[31] A.S. Wills, VaList Version 3.0.13, University College London, UK, 1998–2008. Program available from ⟨www.ccp14.ac.uk⟩.
[32] I.D. Brown, D. Altermatt, Acta Crystallogr. B 41 (1985) 244.
[33] N.E. Brese, M. O'Keeffe, Acta Crystallogr. B 47 (1991) 192.
[34] R. Hoppe, S. Voigt, H. Glaum, J. Kissel, H.P. Müller, K.J. Bernet, Less-Common Met. 156 (1989) 105.
[35] R. Hoppe, Angew. Chem. 78 (1966) 52;
R. Hoppe, Angew. Chem. Int. Ed. 5 (1966) 96.
[36] R. Hoppe, Angew. Chem. 82 (1970) 7;
R. Hoppe, Angew. Chem. Int. Ed. 9 (1970) 25.
[37] R. Hübenthal, MAPLE—Program for the Calculation of MAPLE Values, Version 4, University of Gießen, Gießen, Germany, 1993.
[38] H.R. Hoekstra, Inorg. Chem. 5 (1966) 754.
[39] S.V. Berger, Acta Crystallogr. 5 (1952) 389.
[40] J.P. Laperches, P. Tarte, Spectrochim. Acta 22 (1966) 1201.
[41] H. Böhlhoff, U. Bambauer, W. Hoffmann, Z. Kristallogr. 133 (1971) 386.
[42] K. Machida, H. Hata, K. Okuna, G. Adachi, J. Shiokawa, J. Inorg. Nucl. Chem. 41 (1979) 1425.
[43] A. Haberer, H. Huppertz, unpublished results.